Egyptian Journal of Medical Human Genetics

RESEARCH Open Access

In silico investigations on curcuminoids from *Curcuma longa* as positive regulators of the Wnt/β-catenin signaling pathway in wound healing

Riyan Al Islam Reshad[1], Sayka Alam[2], Humaira Binte Raihan[3], Kamrun Nahar Meem[4], Fatima Rahman[1], Fardin Zahid[1], Md. Ikram Rafid[1], S. M. Obaydur Rahman[5], Sadman Omit[6] and Md. Hazrat Ali[1*]

Abstract

Background: *Curcuma longa* (Turmeric) is a traditionally used herb in wound healing. The efficacy of fresh turmeric paste to heal wounds has already been investigated in multiple ethnobotanical studies. Wnt/β-catenin signaling pathway plays a significant role in wound healing and injury repair processes which has been evident in different in vitro studies. This study aims to analyze the potentiality of curcuminoids (curcumin I, curcumin II and curcumin III) from *Curcuma longa* to bind and enhance the activity of two intracellular signaling proteins- casein kinase-1 (CK1) and glycogen synthase kinase-3β (GSK3B) involved in Wnt/β-catenin signaling pathway. This study is largely based on a computer-based molecular docking program which mimics the in vivo condition and works on a specific algorithm to interpret the binding affinity and poses of a ligand molecule to a receptor. Subsequently, drug likeness property, ADME/Toxicity profile, pharmacological activity, and site of metabolism of the curcuminoids were also analyzed.

Results: Curcumin I showed better affinity of binding with CK1 (– 10.31 Kcal/mol binding energy) and curcumin II showed better binding affinity (– 7.55 Kcal/mol binding energy) for GSK3B. All of the ligand molecules showed quite similar pharmacological properties.

Conclusion: Curcumin has anti-oxidant, anti-carcinogenic, anti-mutagenic, anti-coagulant, and anti-infective properties. Curcumin has also anti-inflammatory and wound healing properties. It hastens wound healing by acting on different stages of the natural wound healing process. In this study, three curcumins from *Curcuma longa* were utilized in this experiment in a search for a drug to be used in wound healing and injury repair processes. Hopefully, this study will raise research interest among researchers.

Keywords: Curcuminoids (curcumin I, curcumin II and curcumin III), *Curcuma longa*, Casein kinase-1 (CK1), Glycogen synthase kinase-3β (GSK3B), Wnt/β-catenin

* Correspondence: hazratsust05@gmail.com
[1]Department of Genetic Engineering and Biotechnology, Shahjalal University of Science and Technology, Sylhet, Bangladesh
Full list of author information is available at the end of the article

Background

Wound, wound healing process, and treatments

The skin is the largest organ of the body which acts as a primary protective barrier. Any physical damage on the skin causes exposure of subcutaneous tissue following a loss of skin integrity known as a wound. Wounds provide a moist, warm, and nutritious environment that is suitable for microbial colonization and proliferation [1]. Infected wounds harbor diverse populations of microorganisms. However, in some cases, these microorganisms can be difficult to identify and fail to respond to antibiotic treatment, resulting in chronic non-healing wounds due to biofilm formation [2].

Wound healing takes place by three main events: inflammatory phase, proliferative phase, and maturation and remodeling phase. During the inflammatory phase, there is an influx of inflammatory cells and local Wnt/β-catenin signaling begins to increase [3]. Wnt proteins are glycoproteins that regulate cell proliferation, migration, and specification of cell fate. Wnt proteins are classified according to their ability to promote stabilization of β-catenin in the cytoplasm. The β-catenin-dependent Wnt pathway signals through cytoplasmic stabilization and accumulation of β-catenin in the nucleus to activate gene transcription which leads to cell division and cell proliferation [4]. During the proliferative phase, a scab (eschar) is formed and the wound is reepithelialized. This phase includes an increased local Wnt response, which increases the accumulation of β-catenin in the cytoplasm. Increases in the β-catenin level lead to some gene transcriptions, such as the matrix metalloproteinases, which cause extracellular matrix deposition, angiogenesis, and the recruitment and proliferation of multiple cell types including stem cells, keratinocytes, and fibroblasts. The third phase, the maturation and remodeling phase, is characterized by extensive extracellular matrix remodeling [3, 5].

Lots of treatments for wound care are available in the market. One of the most commonly used is the standard wound healing technique and wound dressing. A wound dressing includes a cover membrane comprising a semipermeable material with an adhesive-coated skin contact surface. An intermediate layer of material may be placed between the wound and the membrane contact surface for either absorbing fluids from the wound, e.g., with a hydrocolloid or hydrophilic material, or for passing such fluids to the opening with a synthetic material, e.g., rayon [6]. On other hand, the standard wound healing technique includes wet-to-dry dressings, gel, and silver sulfadiazine (Slivadene). Another method is vacuum-assisted closure (VAC) therapy, which is most effective than standard wound healing. This therapy accelerates the healing process by removal of edema and stimulation of mitosis through cell deformation. The success of the treatment depends on the condition of the wound [7]. One percent silver sulfadiazine, an antimicrobial topical ointment, is one of the popular medicine in the treatment of burn wounds around the world. It is easy and convenient to use and causes no pain with low toxicity and sensitivity. Studies have shown that this drug also causes side effects such as reduction of white blood cells, toxic epidermal necrolysis, increased skin pigmentation, neutropenia, increased bacterial resistance, and the skin appearance would not return to normal. For some countries, like Iran, raw materials are often needed to be imported at higher prices [8]. Moreover, an estimated US $25 billion is spent annually only in the USA for wound healing purposes and the margin is increasing day by day due to the increasing healthcare cost. While current therapeutic agents have lower efficacy and many adverse side effects, medicinal plants which have been used as medicine from very ancient times have been proven effective and safe for wound healing, and thus, herbal medicine can be a lucrative alternative to current therapeutic agents [9]. Turmeric is widely used in food as a spice, preservative, and coloring agent. Numerous studies have been conducted with turmeric over the last few decades which have proven its multiple functions in combating multiple diseases. It contains sabinene, borneol, zingiberene, and some other major phytochemicals of great therapeutic value as well as curcuminoid which are responsible for the yellow color of turmeric and it comprises curcumin I, II, and III [10, 11]. The role of both turmeric and individual curcumin from the plant in wound healing has already been demonstrated in laboratory experiments [10, 12].

The Wnt/β-catenin pathway and its involvement in wound healing

The Wnt/β-catenin signaling pathway is activated by the binding of secreted Wnt proteins to a receptor complex containing a member of the FZD family and LRP5/6 [13]. A number of complex proteins facilitate the Wnt/β-catenin pathway. Casein kinase-1 (CK1) and glycogen synthase kinase-3β (GSK3B) phosphorylate several important components like B-catenin, Axin, and APC (adenomatous polyposis coli), in the Wnt/β-catenin signaling pathway and act as either negative or positive regulators of the pathway. These phosphorylation events result in tighter association of Axin and APC with b-catenin CK1 is a family of serine/threonine-specific protein kinases that regulates diverse cellular processes like Wnt signaling [14]. They phosphorylate several pathway components and exert a dual function, acting as both Wnt activators and Wnt inhibitors. The CK1 family consists of six human isoforms (α, δ, ε, γ1, γ2, γ3) which are ubiquitously expressed and share a highly homologous kinase domain, flanked by variable N-

terminal and C-terminal extensions. The amino-terminal kinase domain is highly conserved in all CK1 family members [13, 15]. The serine/threonine kinase GSK3B binds to and phosphorylates several proteins in the Wnt pathway and is serving to the downregulation of β-catenin. As a negative regulator of Wnt signaling, GSK3B would be qualified as a potential tumor suppressor [16].

Wnt/β-catenin pathway in absence of Wnt ligand

In the absence of the Wnt ligand, β-catenin is phosphorylated and targeted to degradation by a protein complex consisting of several molecules including Axin, APC, CK1, and GSK3B. Axin is a protein which serves as a scaffold for the formation of the destruction complex (Fig. 1) [17]. APC is a large protein that interacts with both β-catenin and Axin. It contains three Axin-binding motifs that are interspersed between a series of 15 and 20 amino acid repeats [18]. The scaffolding protein Axin and tumor suppressor APC form a β-catenin destruction complex that binds cytosolic β-catenin and sequentially phosphorylate specific N-terminal residues of β-catenin by serine/threonine kinases, casein kinase 1γ (CK1γ) and glycogen synthase kinase 3β (GSK3B) [19, 20]. Once β-catenin is held into the destruction complex by APC and phosphorylated by GSK3B, the phosphorylated β-catenin is a target for β-Trcp which is a E3-ubiquitin ligase. β-Trcp transfers the ubiquitin chain to the β-catenin and ubiquitinated β-catenin degrades via the ubiquitin proteasome-mediated pathway [18, 21]. In the nucleus, the Wnt target genes are bound by transcription factors of TCF/ LEF. In the absence of β-catenin, these TCF/ LEF transcription factors are bound to Groucho which is a transcriptional repressor which does not allow the Wnt target genes to express [22, 23].

The Wnt/β-catenin pathway in presence of the Wnt ligand

In presence of the Wnt ligand, the Wnt signaling cascade is triggered upon binding of members of the Wnt family proteins to a co-receptor complex, including frizzled (Fz, a G protein-coupled receptor-like protein) and LRP5 or LRP6 (Fig. 2). The signal is transmitted through recruitment of several proteins to the C-terminal intracellular moieties of the activated Fz and LRP5/6 coreceptors. From this point, binding the Wnt ligand to the frizzled receptor leads to dimerization of LRP 5/6 with the frizzled receptor. Disheveled (DVL), a cytoplasmic binding protein which binds to the frizzled receptor, leads to instability of the destruction complex [24]. Dishevelled (Dvl) is recruited and post-translationally modified, depending on the specific nature of the Wnt and of the Fz that are complexed with LRP5/6. Three independent pathways can be activated: canonical, noncanonical, or Ca2 [25]. This unstable destruction complex cannot hold β-catenin any longer. As APC cannot hold β-catenin, β-catenin is no longer phosphorylated by GSK3B and the B-Trcp protein cannot add the ubiquitin chain to β-catenin. Thus, β-catenin is released to the cytosol and the amount of β-catenin in the cytosol increases [23, 26]. β-catenin migrates to the nucleus and replaces the Groucho repressor. The interaction of β-catenin with the N terminus of Tcf converts it into an activator, translating the Wnt signal into the transient transcription of Tcf target genes [27]. β-catenin also recruits CBP and Brg1. These are transcriptional activators that activate the transcription of Wnt-ligand-targeted genes. These Wnt-targeted genes help in cell cycle progression from the G1 phase to the S phase, which leads to cell division and cell proliferation of stem cells, keratinocytes, and fibroblasts. The activation of the Wnt pathway has a key role in fibroblast activation and collagen

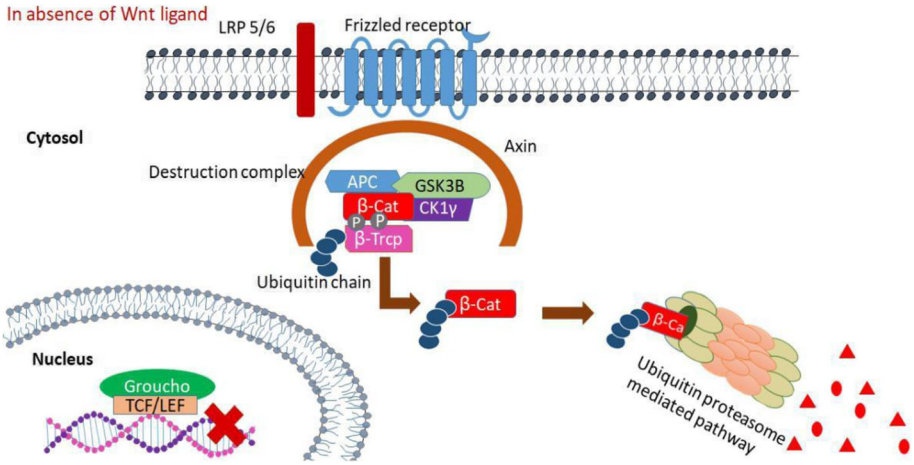

Fig. 1 In the absence of Wnt proteins, Axin, APC, β-catenin, and GSK3B form a complex, in which β-catenin is phosphorylated by CK1 and GSK3B, leading to β-catenin degradation via ubiquitin proteasome-mediated pathway

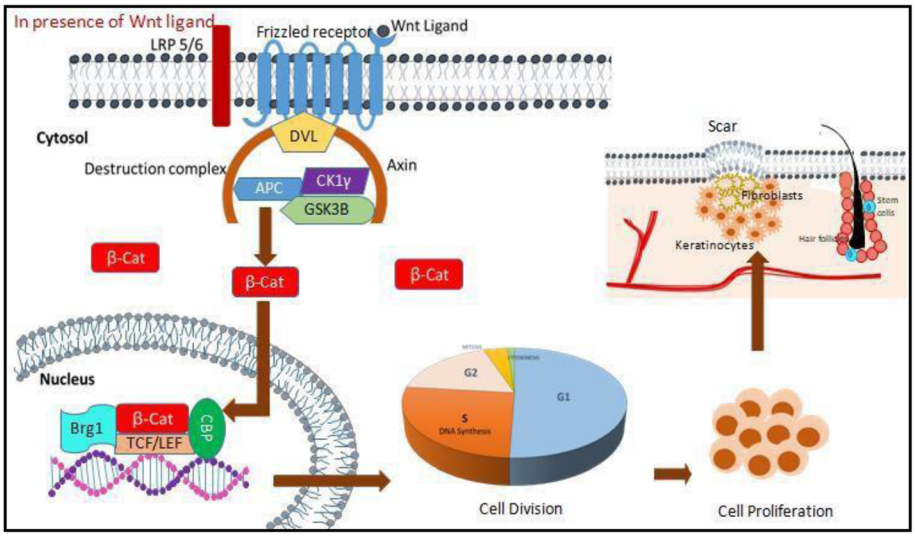

Fig. 2 Wnt proteins bind to Frizzled (Fz) and LRP-5, Axin is recruited to the membranes. The interaction between Axin and LRP-5 may prevent Axin from participating in the degradation of β-catenin. Dvl may also receive signals from the Fz/LRP complex, resulting in the inhibition of GSK3B. β-catenin is not degraded, which eventually leads to transcription of the Wnt-targeted gene, which results in the following events like cell division, cell proliferation, and cell migration to the wound site

release in fibrosis. Wnt signaling stimulated the differentiation of resting fibroblasts into myofibroblasts, increased the release of extracellular matrix components, and induced fibrosis. Stem cells, fibroblasts, and keratinocytes migrate to the wounded site as an immune response. As a result, scarring develops at the wound site and the injury is repaired [3, 21, 28].

In this experiment, curcumin I, II and III (Fig. 3) have been docked with two intended targets of the Wnt/ β-catenin signaling pathway-CK1 and GSK3B (Fig. 4) based on the hypothesis that, these phytocompounds might bind to the targets and act as positive regulators of those targets which may lead to increased signaling and eventually effective wound healing process. Later on, drug likeness property, ADME/Toxicity test, pharmacological activity, and site of metabolism of the selected phytocompounds were also analyzed.

Methods

Molecular docking

Protein preparation

Three-dimentional structures of casein kinase 1 gamma and glycogen synthase kinase-3 beta were downloaded in PDB format from Protein Data Bank (www.rcsb.org). The structures were then prepared and processed using the Protein Preparation Wizard in Maestro Schrödinger Suite (v11.4) [29]. Bond orders were assigned to the structures; hydrogens were added to heavy atoms. All of the water molecules were erased from the atoms and selenomethionines were changed over to methionines. At last, the structures were refined and after that minimized utilizing default Optimized Potentials for Liquid Simulations force field (OPLS_2005). Minimization was performed setting the greatest substantial particle RMSD (root mean square deviation) to 30 Å and any extraordinary water under 3H bonds to non-water was again eradicated during the minimization step.

Ligand preparation

The 3D conformations of curcumin I (PubChem CID: 969516), curcumin II (PubChem CID: 5469424) and curcumin III (PubChem CID: 5315472) were downloaded from PubChem (www.pubchem.ncbi.nlm.nih.gov). These structures were then processed and prepared using the LigPrep wizard of Maestro Schrödinger suite [30]. Minimized 3D structures of ligands were generated using Epik2.2 within pH 7.0 +/− 2.0. Minimization was again carried out using OPLS_2005 force field which generated a maximum of 32 possible stereoisomers depending on available chiral centers on each molecule.

Receptor grid generation

Grid usually restricts the active site to a specific area of the receptor protein for the ligand to dock specifically within that area. In Glide, a grid was generated using default van der Waals radius scaling factor 1.0 and charge cutoff 0.25 which was then subjected to Optimized Potentials OPLS_2005 force field for the minimized structure. A cubic box was generated around the active site (reference ligand active site) of target molecules. Then the grid box dimension was adjusted to 10 Å × 10 Å × 10 Å for docking to be carried out.

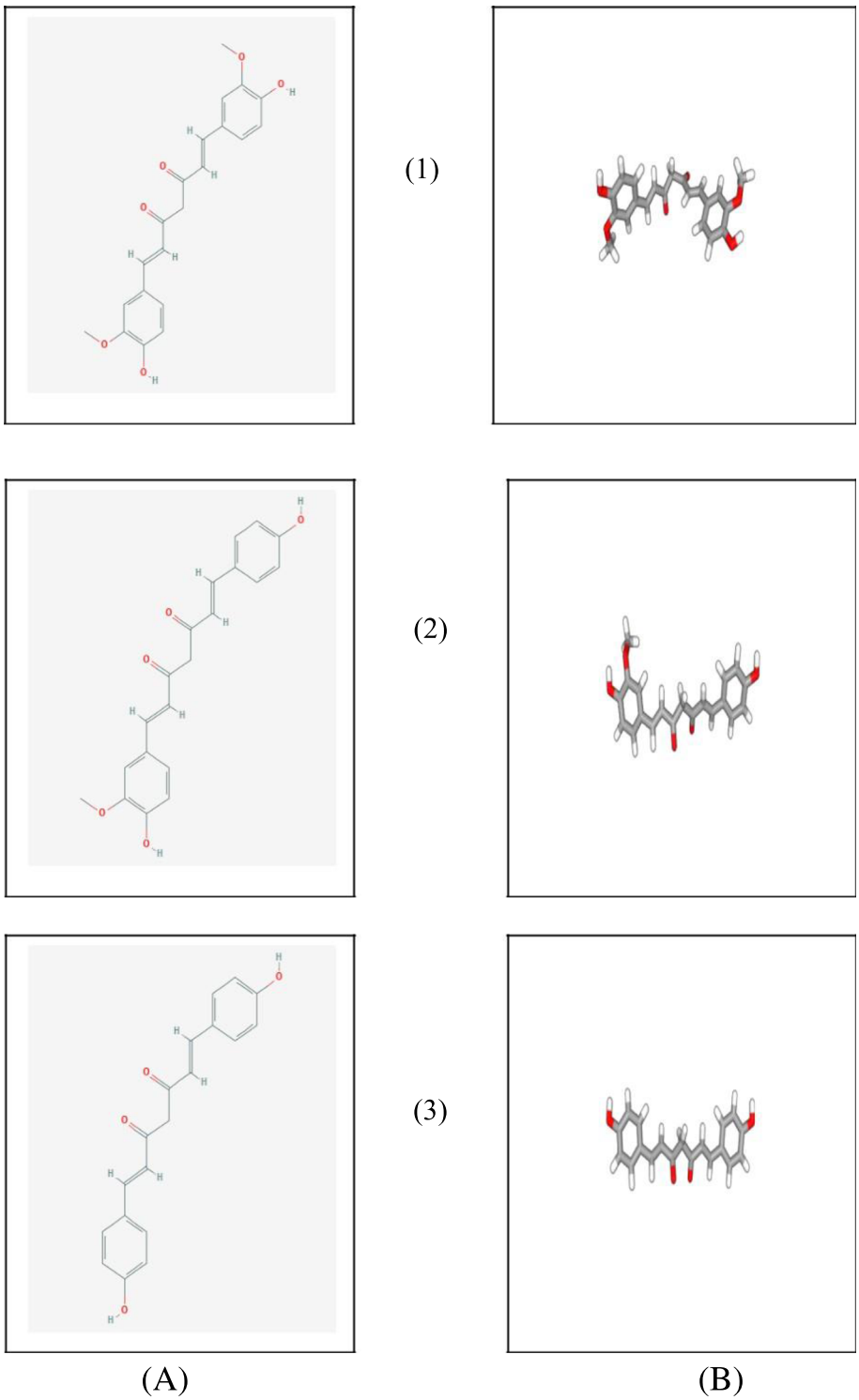

Fig. 3 Structures of (1) curcumin I (PubChem CID: 969516), (2) curcumin II (PubChem CID: 5469424), and (3) curcumin III (PubChem CID: 5315472); (**A**) 2D, (**B**) 3D

Glide standard precision ligand docking

Standard precision (SP) adaptable glide docking was carried out using Glide in Maestro Schrödinger [31]. The van der Waals radius scaling factor and charge cutoff were set to 0.80 and 0.15 respectively for all the ligand molecules under study. The final score was assigned

Fig. 4 Three dimension structure of (**A**) casein kinase-1 (PDB Id: 2IZS) and (**B**) glycogen synthase kinase-3β (PDB Id: 3F88) in their native ligand-bound form. Receptors are represented in cartoon style and ligands are represented in ball and stick style

according to the pose of the docked ligand within the active site of the receptor molecules. The docking result is summarized in Table 1. The best possible poses and types of ligand-receptor interactions (Figs. 5 and 6) were analyzed utilizing Discovery Studio Visualizer [32].

Structure-based drug likeness property and ADME/toxicity prediction

The molecular structures of every ligand were analyzed using SWISSADME server (https://swissadme.ch) in order to confirm whether the physicochemical properties like molecular weight, hydrogen bond donor, hydrogen bond acceptor, molar refractivity, etc. of ligands follow Lipinski's rule of five or not [33]. Additional physicochemical properties such as topological polar surface area, number of rotatable bonds, drug score, drug likeness score, etc. of ligand molecules were again calculated using OSIRIS property explorer (https://organic-chemistry.org/prog/peo/) [34]. The result of drug likeness property analysis is summarized in Table 2. The ADME/T profile for each of the ligand molecules was analyzed using the online-based server admetSAR (https://lmmd.ecust.edu.cn/admetsar1/predict/) to predict their various pharmacokinetic and pharmacodynamic properties including blood-brain barrier permeability, human abdominal adsorption, AMES toxicity, Cytochrome P (CYP) inhibitory promiscuity, carcinogenicity, mutagenicity, Caco-2 permeability, etc. [35]. The result of ADME/T for all the ligand molecules is represented in Table 3.

Structure-based pharmacological activity and P450 site of metabolism prediction

Biological activities of each ligand molecule were predicted using the PASS (Prediction of Activity Spectra for Substances) online server (http://www.pharmaexpert.ru/passonline/) [36]. All of the ligand molecules were analyzed with respect to the probability of activity (Pa) and inactivity (Pi) for 25 intended biological activities depending on their structure. Results of PASS prediction are summarized in Table 4. P450 site of metabolism of each ligand molecule was predicted using SMARTcyp online server (https://smartcyp.sund.ku.dk/mol_to_som) in order to analyze which atoms in the molecule are more prone to metabolism by cytochrome P450 family of enzymes—CYP3A4, CYP2D6, CYP2C9—based on the specific ligand structure [37]. The result of the cytochrome P450 site of metabolism prediction is summarized in Table 5 and Fig. 7.

Result

Molecular docking

All of the selected ligand molecules docked successfully with both CK1 and GSK3B with notable binding energies (Table 1). Curcumin I docked with a binding energy of − 10.31 Kcal/mol within the binding site of CK1. It formed 1 conventional hydrogen bond with Glu117 with 1.62 Å distance apart and 2 conventional hydrogen bonds with Leu119 with 1.99 Å and 2.44 Å distance apart respectively in the binding site backbone of CK1. In addition, curcumin I also formed two non-conventional hydrogen bonds with Lys72 and Gly140. Moreover, it interacted with 10 amino acid residues in total along with Pi-alkyl (hydrophobic) and Pi-anion (electrostatic) interactions. On the contrary, curcumin I interacted with GSK3B with slightly lower energy (− 7.533 kcal/mol) than CK1 within the binding pocket. It formed 2 conventional hydrogen bonds with Lys85 at 2.22 Å and 2.84 Å distance apart and 1 conventional hydrogen bond with Val135 at 2.54 Å distance apart inside the binding site of GSK3B. Curcumin I interacted with 8 amino acid residues within the binding site of GSK3B and notably with other additional types of interactions like Pi-sulfur, Pi-alkyl interactions. It also formed 2 non-conventional hydrogen bonds with Pro136 and Asp200 with GSK3B.

Curcumin II docked to CK1 with a binding energy of − 7.826 Kcal/mol. It formed 4 conventional hydrogen bonds—2 with Leu119 at 1.99 Å and 2.79 Å distance apart and 1 with Glu117 and Asp125 each at 1.84 Å and 2.09 Å distance apart respectively within the binding site

Table 1 Result of molecular docking between curcumin I (PubChem CID: 969516), curcumin II (PubChem CID: 5469424), curcumin III (PubChem CID: 5315472), and CK-1 (PDB Id: 2IZS) and GSK3B (PDB Id: 3F88)

Compound name	Receptor	Binding energy (Kcal/mol)	Interacting amino acids	Bond distance (Å)	Interaction category	Type of interaction
Curcumin I	CK1	− 10.31	Leu57	5.26	Hydrophobic	Pi-alkyl
			Lys72	2.3	**Hydrogen bond**	Non-conventional
			Ala70	4.01	Hydrophobic	Pi-alkyl
			Ile184	4.87	Hydrophobic	Pi-alkyl
			Leu116	5.36	Hydrophobic	Pi-alkyl
			Asp185	3.66	Electrostatic	Pi-Anion
			Glu117	1.62	**Hydrogen bond**	Conventional
			Leu119	1.99	**Hydrogen bond**	Conventional
			Gly120	3.01	**Hydrogen bond**	Non-conventional
			Leu169	5.36	Hydrophobic	Pi-alkyl
			Leu119	2.44	**Hydrogen bond**	Conventional
	GSK3B	− 7.533	Lys85	2.22	**Hydrogen bond**	Conventional
			Lys85	2.84	**Hydrogen bond**	Conventional
			Val70	5.11	Hydrophobic	Pi-alkyl
			Leu132	4.95	Hydrophobic	Pi-alkyl
			Val135	2.54	**Hydrogen bond**	Conventional
			Pro136	2.93	**Hydrogen bond**	Non-conventional
			Val110	5.38	Hydrophobic	Pi-alkyl
			Cys199	3.73	Others	Pi-sulfur
			Asp200	2.56	**Hydrogen bond**	Non-conventional
Curcumin II	CK1	− 7.826	Glu117	1.84	**Hydrogen bond**	Conventional
			Leu119	1.99	**Hydrogen bond**	Conventional
			Leu169	5.25	Hydrophobic	Pi-alkyl
			Ala70	4.13	Hydrophobic	Pi-alkyl
			Asp125	2.09	**Hydrogen bond**	Conventional
			Ile184	4.84	Hydrophobic	Pi-alkyl
			Lys72	2.54	**Hydrogen bond**	Non-conventional
			Leu119	2.79	**Hydrogen bond**	Conventional
			Leu57	5.08	Hydrophobic	Pi-alkyl
	GSK3B	− 7.588	Ile62	4.91	Hydrophobic	Pi-alkyl
			Val70	4.59	Hydrophobic	Pi-alkyl
			Lys85	1.87	**Hydrogen bond**	Conventional
			Arg141	4.05	Electrostatic	Pi-cation
			Val135	2.05	**Hydrogen bond**	Conventional
			Tyr134	2.39	**Hydrogen bond**	Non-conventional
			Lys85	2.97	**Hydrogen bond**	Conventional
			Cys199	3.73	Others	Pi-sulfur
			Asp200	2.71	**Hydrogen bond**	Non-conventional
Curcumin III	CK1	− 6.356	Pro333	4.37	Hydrophobic	Pi-alkyl
			Thr332	2.71	**Hydrogen bond**	Conventional
			Leu118	2.71	**Hydrogen bond**	Non-conventional
			Leu119	2	**Hydrogen bond**	Conventional
	GSK3B		Ile62	4.48	Hydrophobic	Pi-alkyl

Table 1 Result of molecular docking between curcumin I (PubChem CID: 969516), curcumin II (PubChem CID: 5469424), curcumin III (PubChem CID: 5315472), and CK-1 (PDB Id: 2IZS) and GSK3B (PDB Id: 3F88) *(Continued)*

Compound name	Receptor	Binding energy (Kcal/mol)	Interacting amino acids	Bond distance (Å)	Interaction category	Type of interaction
		– 6.618	Val70	4.75	Hydrophobic	Pi-alkyl
			Lys60	1.93	**Hydrogen bond**	Conventional
			Lys85	5.11	Hydrophobic	Pi-alkyl
			Cys199	4.12	Hydrophobic	Pi-alkyl

of CK1. Moreover, it also formed 1 non-conventional hydrogen bond with Lys72 in the binding pocket backbone. Curcumin II interacted with 8 amino acid residues in total with additional hydrophobic (Pi-alkyl) binding interactions. Conversely, curcumin II showed a subtle lower binding energy (– 7.588 kcal/mol) with GSK3B. In the binding site backbone of GSK3B it formed 2 conventional hydrogen bonds with Lys85 at 1.87 Å, 2.97 Å distance apart and another conventional hydrogen bond with Val135 at 2.05 Å distance apart. Curcumin II also formed 2 non-conventional hydrogen bonds with Tyr134 and Asp200 within the binding site of GSK3B.

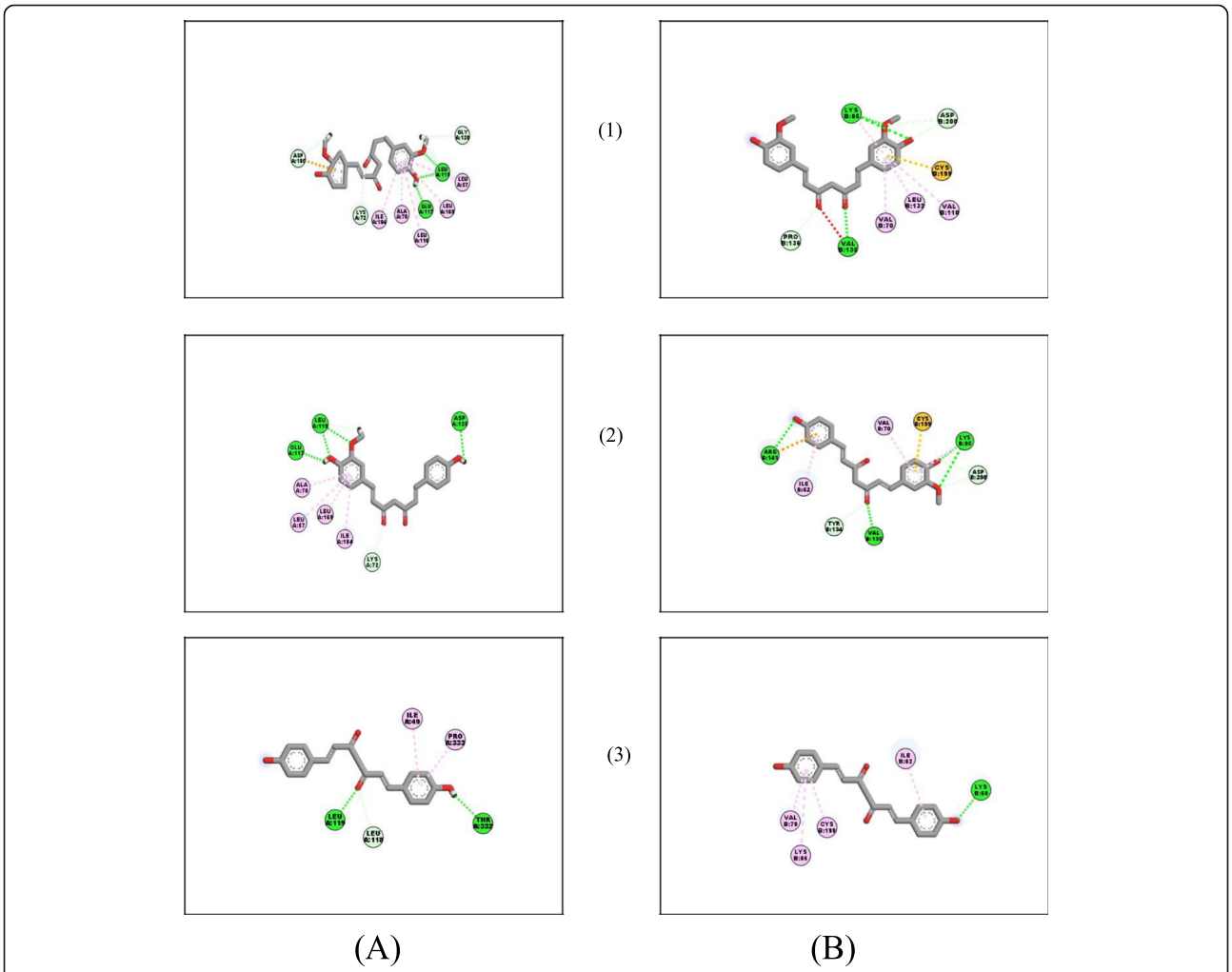

Fig. 5 2D representation of ligand-receptor interactions between (1) curcumin I (PubChem CID: 969516), (2) curcumin II (PubChem CID: 5469424), and (3) curcumin III (PubChem CID: 5315472) and (**A**) casein kinase-1 (PDB Id: 2IZS) and (**B**) glycogen synthase kinase-3β (PDB Id: 3F88). Ligand is represented as a stick and interacting amino acid (labeled) of the receptor is represented as a disc sphere. The dotted line represents the type of interactions: dark green: hydrogen bond; light green: van der Waals interaction; pink: Pi-alkyl interaction; white: carbon-hydrogen bond; red: acceptor-acceptor interaction; orange: Pi-sulfur interaction

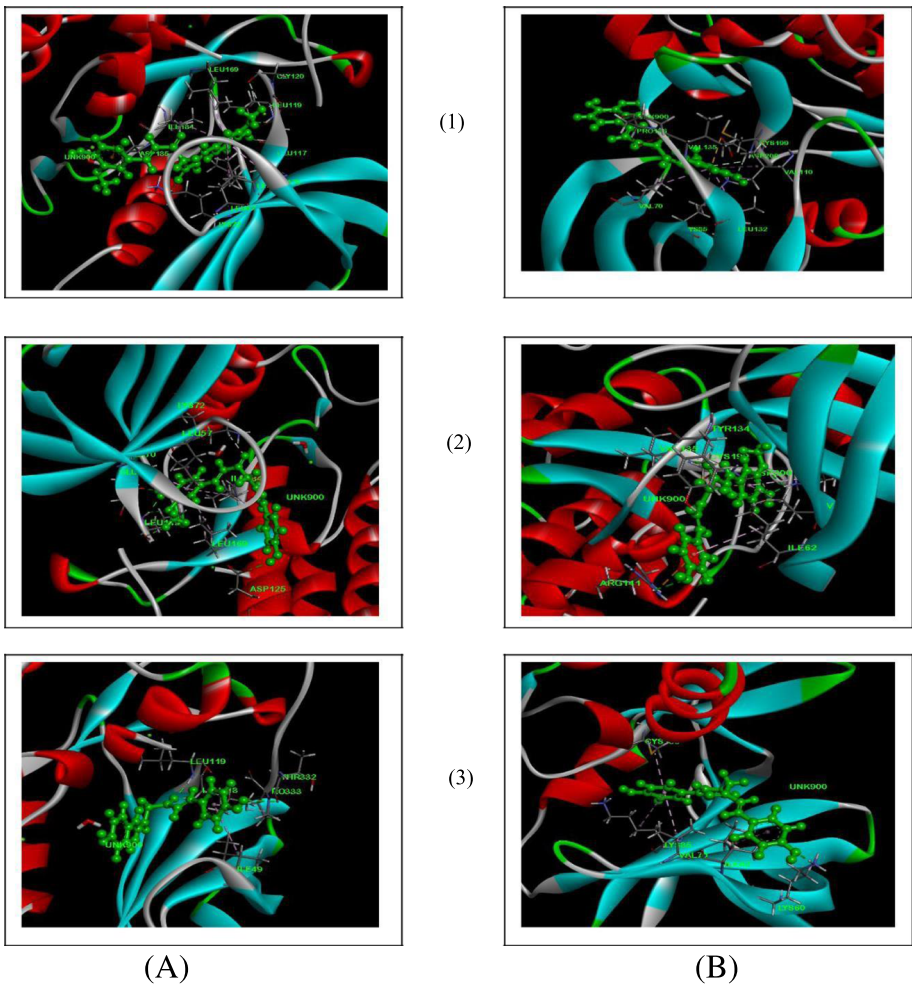

Fig. 6 3D representation of the best possible poses and ligand-receptor interactions between (1) curcumin I (PubChem CID: 969516), (2) curcumin II (PubChem CID: 5469424), and (3) curcumin III (PubChem CID: 5315472) and (A) casein kinase-1 (PDB Id: 2IZS) and (**B**) glycogen synthase kinase-3β (PDB Id: 3F88). Ligand (UNK: 900) is represented as a ball and stick and the interacting amino acid (labeled) of the receptor is represented in a stick style. The receptor is represented in ribbon style. The dotted line represents the type of interactions: green: hydrogen bond; pink: Pi-alkyl interaction; white: carbon-hydrogen bond; red: acceptor-acceptor interaction; orange: Pi-sulfur interaction

With additional Pi-alkyl, Pi-cation, and Pi-sulfur bonding interactions curcumin II interacted with 8 amino acid residues in total.

Curcumin III docked successfully with CK1 with – 6.356 kcal/mol binding energy. It formed 2 conventional hydrogen bonds with Leu119 and Thr332 at 2.00 Å and 2.71 Å distance apart respectively within the binding pocket. It also formed 2 non-conventional hydrogen bonds with Leu118 and Pro333. Curcumin III interacted with 5 amino acids in total with one hydrophobic interaction (Pi-alkyl) with Pro333. On the other hand, curcumin III docked with GSK3B with slightly higher binding energy (– 6.618 kcal/mol). It formed just 1 conventional hydrogen bond with Lys60 at 1.93 Å distance apart. In addition, it interacted with a total of 5 amino acid residues inside the binding pocket of GSK3B only with Pi-Alky hydrophobic interaction. Curcumin III did not show any non-conventional hydrogen bonding with any amino acid residues.

Drug likeness property

The results of the drug likeness property analysis are summarized in Table 2. All of the selected ligand molecules followed Lipinski's rule of five with respect to molecular weight (acceptable range: ˂ 500), number of hydrogen bond donors (acceptable range: ≤ 5), number of hydrogen bond acceptors (acceptable range: ≤ 10), lipophilicity (expressed as LogP, acceptable range: ˂ 5), and molar refractivity (40–130) [38]. Curcumin III showed the lowest topological polar surface area (TPSA) of 74.60 $Å^2$ followed by curcumin II (83.83 $Å^2$) and curcumin I (93.06 $Å^2$). Again, curcumin III showed the lowest LogS value (– 3.80) among the three ligand molecules. Curcumin II (– 3.92) and curcumin I (–

Table 2 Result of drug likeness property analysis of curcumin I (PubChem CID: 969516), curcumin II (PubChem CID:5469424), and curcumin III (PubChem CID: 5315472). Lipinski's rule of five: molecular weight: < 500, number of H-bond donors: ≤ 5; number of H-bond acceptors: ≤ 10; lipophilicity (expressed as LogP): < 5; and molar refractivity: 40–130

Drug likeness properties	Curcumin I	Curcumin II	Curcumin III
Molecular weight	368.38 g/mol	338.35 g/mol	308.33 g/mol
LogP	3.27	2.78	1.75
LogS	− 3.94	− 3.92	− 3.8
H-bond acceptor	6	5	4
H-bond donor	2	2	2
Molar refractivity	102.8	96.31	89.82
Heavy atoms	27	12	23
TPSA	93.06 $Å^2$	83.83 $Å^2$	74.60 $Å^2$
Rotatable bonds	8	8	6
Drug likeness score	− 2.63	− 3.55	− 4.48
Drug score	0.53	0.41	0.41

3.934) showed almost similar LogS values. Curcumin I showed the highest drug likeness score (− 2.63) followed by curcumin II (− 3.55) and curcumin III (− 4.48). Curcumin II and curcumin III showed the same drug score (0.41) whereas curcumin I showed the highest drug score (0.53) among the ligand molecules. Curcumin I and II have 8 rotatable bonds and on the contrary, Curcumin III has 6 rotatable bonds. Curcumin I, II, and III have 27, 12, and 23 heavy atoms respectively.

ADME/T Test

Results of ADME/T test are summarized in Table 3. All the selected ligand molecules showed blood-brain barrier and Caco2 cell membrane permeability. All of them showed positive indication of human intestinal absorption. Curcumin I and II are substrates of cell membrane P-glycoprotein whereas curcumin III is a non-substrate. All of them are non-substrate for CYP450 3A4, CYP450 2C9, and CYP450 2D6 metabolic enzymes. Curcumin II and III are non-inhibitors of CYP450 2D6 whereas curcumin I is an inhibitor. All of the selected ligand molecules are inhibitors of CYP450 1A2, CYP450 2C9, and CYP450 2C19 metabolic enzymes. All of the selected ligand molecules exhibited high CYP450 inhibitory promiscuity, no AMES toxicity, and non-carcinogenicity. All of them are not readily biodegradable and showed type III acute oral toxicity.

Pharmacological Activity Prediction

The results of pharmacological activity prediction are summarized in Table 4. Curcumin I, II, and III were analyzed for 25 intended biological activities. All selected ligand molecules showed almost similar pharmacological

Table 3 ADME/T properties of curcumin I (PubChem CID: 969516), curcumin II (PubChem CID: 5469424) and curcumin III (PubChem CID: 5315472). BBB+: capable of penetrating the blood-brain barrier (BBB); HIA+: absorbed in human intestinal tissue; Caco-2+: permeable through the membrane of Caco-2 cell lines; CYP450: cytochrome P450

Properties	Curcumin I	Curcumin II	Curcumin III
Blood-brain barrier	BBB+	BBB+	BBB+
Human intestinal absorption	HIA+	HIA+	HIA+
Caco-2 Permeability	Caco2+	Caco2+	Caco2+
P-Glycoprotein substrate	Substrate	Substrate	Non-substrate
CYP450 2C9 substrate	Non-substrate	Non-substrate	Non-substrate
CYP450 2D6 substrate	Non-substrate	Non-substrate	Non-substrate
CYP450 3A4 substrate	Non-substrate	Non-substrate	Non-substrate
CYP450 1A2 inhibitor	Inhibitor	Inhibitor	Inhibitor
CYP450 2C9 inhibitor	Inhibitor	Inhibitor	Inhibitor
CYP450 2D6 inhibitor	Inhibitor	Non-inhibitor	Non-inhibitor
CYP450 2C19 inhibitor	Inhibitor	Inhibitor	Inhibitor
CYP450 3A4 inhibitor	Non-inhibitor	Non-inhibitor	Inhibitor
CYP inhibitory promiscuity	High CYP inhibitory promiscuity	High CYP inhibitory promiscuity	Low CYP inhibitory promiscuity
AMES toxicity	Non AMES toxic	Non AMES toxic	Non AMES toxic
Carcinogens	Non-carcinogens	Non-carcinogens	Non-carcinogens
Biodegradation	Not ready biodegradable	Not ready biodegradable	Not ready biodegradable
Acute oral toxicity	III	III	III

Table 4 Pharmacological activities of curcumin I (PubChem CID: 969516), curcumin II (PubChem CID: 5469424), and curcumin III (PubChem CID: 5315472). When Pa > 0.7: compound is very likely to exhibit the activity; when 0.7 > Pa > 0.5: compound is likely to exhibit the activity; when Pa < 0.5: compound is less likely to exhibit the activity

Sl. no.	Biological activity	Curcumin I		Curcumin II		Curcumin III	
		Pa	Pi	Pa	Pi	Pa	Pi
1	Antiallergic	0.435	0.043	0.408	0.05	0.251	0.129
2	Antiinflammatory	0.677	0.019	0.667	0.02	0.704	0.015
3	Antimutagenic	0.814	0.004	0.834	0.003	0.79	0.004
4	Apoptosis agonist	0.803	0.008	0.861	0.005	0.871	0.005
5	Antiulcerative	0.651	0.007	0.65	0.007	0.633	0.009
6	Antioxidant	0.61	0.004	0.624	0.004	0.637	0.004
7	Caspase 3 stimulant	0.747	0.009	0.719	0.01	0.492	0.029
8	Chemopreventive	0.692	0.007	0.718	0.006	0.576	0.011
9	Carminative	0.833	0.003	0.81	0.004	0.822	0.003
10	DNA ligase (ATP) inhibitor	0.314	0.04	0.326	0.036	0.364	0.024
11	Free radical scavenger	0.766	0.003	0.785	0.003	0.67	0.004
12	Fibrinolytic	0.731	0.013	0.735	0.012	0.717	0.017
13	Gluconate 2-dehydrogenase inhibitor	0.833	0.01	0.822	0.012	0.836	0.009
14	Hepatoprotectant	0.469	0.023	0.656	0.009	0.578	0.014
15	HMOX1 expression enhancer	0.826	0.003	0.854	0.003	0.858	0.003
16	Membrane permeability inhibitor	0.724	0.029	0.736	0.025	0.721	0.03
17	Prostate cancer treatment	0.554	0.006	0.555	0.006	0.573	0.005
18	Proliferative disease treatment	0.558	0.014	0.59	0.011	0.553	0.014
19	Reductant	0.864	0.003	0.884	0.003	0.908	0.003
20	Radioprotector	0.559	0.019	0.561	0.019	0.566	0.019
21	Sigma receptor agonist	0.505	0.024	0.521	0.022	0.488	0.027
22	Sugar-phosphatase inhibitor	0.593	0.057	0.555	0.067	0.782	0.019
23	TNF expression inhibitor	0.764	0.004	0.901	0.002	0.825	0.003
24	UDP-glucuronosyltransferase substrate	0.747	0.011	0.775	0.009	0.739	0.012
25	Vasoprotector	0.678	0.012	0.62	0.017	0.654	0.014

activities although their scores varied slightly with respect to specific activity. Curcumin II showed 13 pharmacological activities with a Pa score greater than 0.7 whereas curcumin I and III showed 12 pharmacological activities each with a Pa score greater than 0.7.

P450 Site of Metabolism Prediction

The result of P450 metabolism prediction is summarized in Table 5 and depicted using Figure. Carbon13 and Carbon1 were the most prominent atoms in curcumin I and II which exhibited the lowest enzyme scores for metabolism by 3 isoforms (3A4, 2D6, and 2C9) of the CYP450 family of enzymes. And in the case of curcumin III, Carbon11 showed the lowermost enzyme scores for all the isoforms of metabolic enzymes. However, Carbon2, Carbon6, Carbon22, Carbon23, and Carbon26 also showed satisfactory enzyme scores indicating the probability of being catalyzed by all three enzymes.

Discussion

Medicinal plants are the source of novel phytocompounds which provide numerous therapeutic benefits. Many plant-derived compounds and plant extract have been shown to have wound healing activity [39]. *Curcuma longa* has also shown in a laboratory experiment that it has wound healing properties [4, 40]. The involvement of Wnt signaling and upregulation of this signaling pathway in cutaneous wound healing and injury repair processes have been demonstrated in a laboratory experiment [4, 41]. Molecular docking is a method of estimating the preferred orientation of a small molecule when bound to the binding site of a second molecule. It is one of the most frequently used techniques in structure-based drug designing [42]. Molecular docking works on a specific scoring algorithm and assigns binding energy to the ligand molecules that fit with the target which reflects the binding affinity. The low binding

Table 5 Result of P450 metabolism site prediction. Atoms are ranked on the basis of lowest enzyme score which means the highest probability of being catalyzed by enzyme. *Enzyme Score: Energy - 8*A - 0.04*SASA*. A: Accessibility (not shown) is the relative distance of an atom from the center of molecule. Energy: approximate activation energy required for CYP active site to catalyze particular atom. SASA: solvent accessible surface area means local accessibility of atom. 2DSASA: value calculated from molecular topology

Compounds	Enzymes	Ranking	Atom	Enzyme score	Energy	2DSASA
Curcumin I	CYP3A4	1	C.13	43.6	48.5	22.4
		2	C.26	51.6	62.2	64.3
		3	C.23	66.5	74.1	27.8
	CYP2D6	1	C.1	59.6	62.2	64.3
		2	C.13	74.5	48.5	22.4
		3	C.22	89.5	77.2	28.6
	CYP2C9	1	C.1	59.6	62.2	64.3
		2	C.13	71.3	48.5	22
		3	C.22	87.9	77.2	28.6
Curcumin II	CYP3A4	1	C.13	43.6	48.5	22.4
		2	C.1	51.6	62.2	64.3
		3	C.6	66.5	74.1	27.8
	CYP2D6	1	C.1	59.6	62.2	64.3
		2	C.13	74.5	48.5	22.4
		3	C.22	89.3	77.2	31.3
	CYP2C9	1	C.1	59.6	62.2	64.3
		2	C.13	71.3	48.5	22
		3	C.22	87.7	77.2	31.3
Curcumin III	CYP3A4	1	C.11	43.6	48.5	22.4
		2	C.2	68.9	77.2	31.3
		3	C.1	73.2	80.8	28.6
	CYP2D6	1	C.11	74.5	48.5	22.4
		2	C.2	89.3	77.2	31.3
		3	C.1	99.8	80.8	
	CYP2C9	1	C.11	71.3	48.5	22.4
		2	C.2	87.7	77.2	31.3
		3	C.1	97.4	80.8	28.6

energy of a ligand molecule with the target indicates high stability of the ligand-receptor complex meaning they remain more time in contact [43]. In this study curcuminoids (Fig. 3) (curcumin I, II, and III) from *Curcuma longa* were docked against 2 components (Fig. 4) (casein kinase 1 and glycogen synthase kinase 3 beta) of the Wnt/β-catenin signaling pathway based on the hypothesis that the ligand molecules bind to the target and might augment their activity. In this experiment, curcumin I interacted with CK1 with the lowest binding energy (– 10.311 kcal/mol) and curcumin II interacted with GSK3B with the lowest binding energy (– 7.588 kcal/mol) suggesting the most favorable binding (Table 1). As a consequence curcumin I interacted with the highest number of amino acid residues (10) in the binding site backbone of CK1 and curcumin II interacted with 8 amino acid residues within the binding site of GSK3B (Figs. 5 and 6). Curcumin I also showed almost a similar binding energy (– 7.533 kcal/mol) as with curcumin II for interaction with GSK3B. However, curcumin III showed the highest binding energies for both CK1 and GSK3B binding sites. Hydrogen bonding and hydrophobic interactions play a key role by strengthening the drug-receptor interaction. All of the selected ligand molecules formed a significant number of hydrogen bonds and hydrophobic interactions within the binding site of the target molecules [44].

Drug likeness property evaluation is an important determinant of the successful drug discovery approach. It helps in specifying physicochemical properties of ligand molecules and helps in determining whether a drug should pass the phase I clinical trial or not. In this

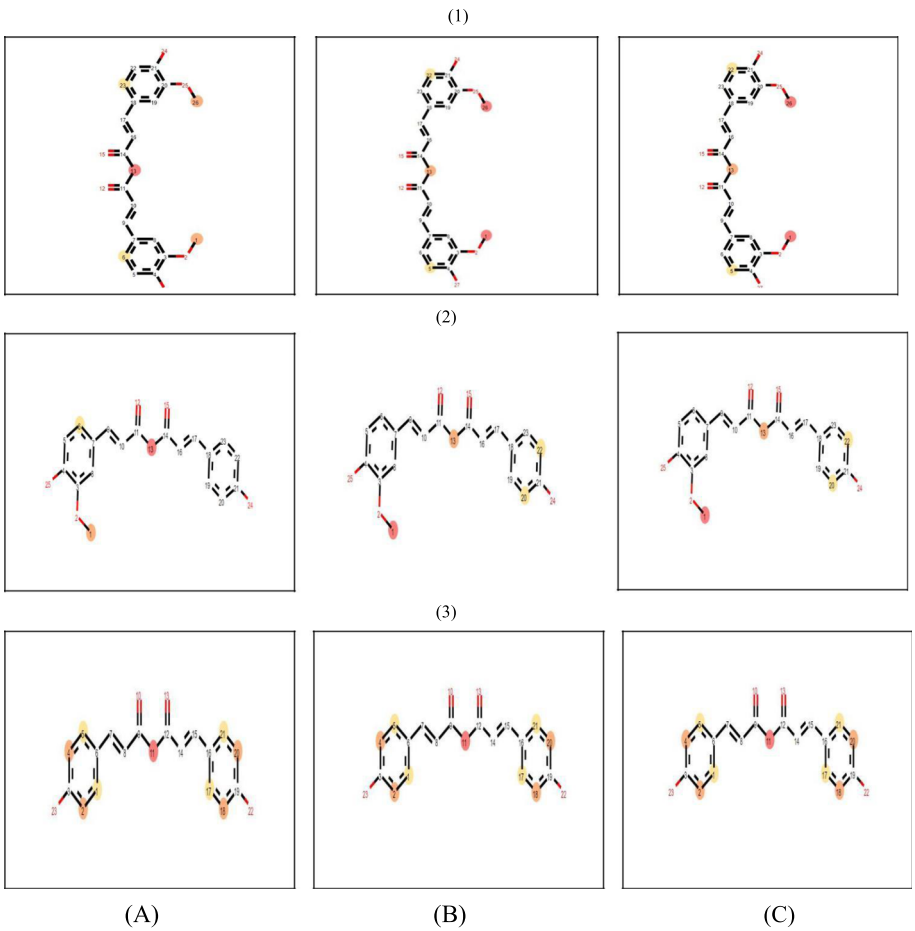

Fig. 7 Representation of best possible atoms (marked in colored spheres) of (1) curcumin I (PubChem CID: 969516), (2) curcumin II (PubChem CID: 5469424), and (3) curcumin III (PubChem CID: 5315472) subjected to metabolism by the CYP450 group of enzymes (**A**) CYP 3A4, (**B**) CYP 2D6, and (**C**) CYP 2C9. Atoms marked in a darker sphere are subjected to have better probability of metabolism by enzymes followed by the ones marked in a lighter sphere

experiment, ligand molecules were examined according to Lipinski's rule of five which states that drugs are likely to have poor bioavailability and lower permeation which violates the rules [38, 45]. All of the selected ligand molecules followed Lipinski's rule of five. Moreover, 10 or fewer rotatable bonds and topological polar surface area equal (TPSA) to or less than 140 $Å^2$ are considered to contribute to better oral bioavailability of the candidate drug molecule [46]. All of the selected ligand molecules have TPSA lower than 140 $Å^2$ and rotatable bonds lower than 10. A higher molecular weight reduces the permeability of a drug through the lipid bilayer and lower ones help in the increment of drug permeability. LogP is expressed in the context of lipophilicity and referred to as the logarithm of partition coefficient of the candidate molecule in organic and aqueous phases. Lipophilicity affects the absorption of the candidate drug molecule inside the human body. Higher LogP is associated with lower absorption of the drug inside the human body and a lower value ensures a higher rate of absorption of the candidate drug molecule. LogS value influences the solubility of the candidate molecule and the lowest value is always preferred for the drug molecule under investigation in a drug discovery approach. The number of hydrogen bond donors and acceptors outside the acceptable range again influences the ability of a drug molecule to cross the bilayer membrane of the cell. All of the selected ligand molecules followed Lipinski's rule of five in this experiment [47, 48]. All selected molecules showed druggable properties within acceptable ranges (Table 2).

The application of in silico ADME/T test has gained the attention of researchers over the last decade. In silico investigation of adsorption, distribution, metabolism, and toxicity has enhanced the in vitro ADME/T test and thus has reduced the time and cost along with increasing the success rate of the drug discovery approach [49–56]. Blood-brain barrier permeability becomes a major concern when drugs target primarily the cells of the central

nervous system (CNS). The oral delivery system is the most commonly used route of drug administration and the administered drug passes through the digestive tract so it is appreciable that the drug is highly absorbed in human intestinal tissue. P-glycoproteins are embedded on the cell membrane and facilitate the transport of many drugs inside the cell and therefore its inhibition may affect the normal drug transport. In vitro study of drug permeability test utilizes Caco2 cell line and its permeability to the intended candidate drug molecule reflects that the drug is easily absorbed in the intestine [57–59]. All curcumin analogues were reported to be non-inhibitory to P-glycoprotein, permeable through the blood-brain barrier, absorbable in the human intestinal tissue, and permeable through membrane Caco2 cell lines. The cytochrome P450 family of enzymes plays a major role in drug interaction, metabolism, and excretion inside the body. Inhibition of these enzymes may lead to the elevation of drug toxicity, slow clearance, and malfunction of the drug compound [60]. The inhibitory effect of all three curcumin analogues was observed against multiple enzymes which may lead to poor degradability and slow excretion of those compounds inside the human body. The acute oral toxicity is expressed in terms of median lethal dose (LD50), the dose that is capable of killing 50% of the animals under study within 24 h. Chemicals can be classified into 4 categories (I to IV) based on their extent to induce oral toxicity: toxicity category I is highly toxic and irritant, toxicity category II is moderately toxic and irritant, toxicity category III is slightly toxic and irritant, and toxicity category IV is basically non-toxic and does not irritate [61, 62]. Mutagenicity is considered one of the most common end point of toxicity. AMES toxicity examines the toxicity of chemicals [63, 64]. None of the selected ligand molecules showed AMES toxicity and carcinogenicity (Table 3).

Prediction of Activity Spectra for Substances (PASS) predicts the biological activity spectrum of a compound based on its native structure. PASS predicts the activity of a compound based on Structure-Activity Relationship Base (SAR Base) which assumes that the activity of a compound is related to its structure. It functions by comparing the 2D structure of a compound relative to another well-known compound having biological activities existing in the database with almost 95% accuracy [65]. It predicts the result in the context of probability of activity (Pa) and Probability of inactivity (Pi) of a compound and the result varies between 0.000 and 1.000. When Pa > Pi only then the activity is considered possible for a compound [66]. When Pa > 0.7, then the compound is very likely to exhibit the activity but the possibility of the compound being an analogue to a known pharmaceutical is also high. When 0.5 < Pa < 0.7, then the compound is likely to exhibit the activity but the probability is less along with the chance of being a known pharmaceutical agent is also lower. When Pa < 0.5, then the compound is less likely to exhibit the activity [67]. Curcumin II was reported to be more biologically active than the other two compounds for 25 selected activities (Table 4).

The cytochrome P450 (CYP450) family comprises 57 isoforms of enzymes responsible for xenobiotic metabolism inside the human body. So, rigorous testing of the compound's probability of being metabolized by the CYP450 enzymes is a prerequisite for the drug discovery approach. The in silico approach for CYP450 utilizes the 2D structure of a compound to determine which site in a molecule is more liable to metabolism by CYP450 enzymes [68, 69]. Curcumin I showed a better result in the P450 site of metabolism prediction (Table 5) (Fig. 7).

All the selected ligand molecules docked successfully with both targets and therefore all of them might have roles in wound healing. However, curcumin I showed the highest affinity of binding (– 10.311 kcal/mol) with CK1 and curcumin II showed the highest affinity of binding (– 7.588 kcal/mol) with GSK3B which may indicate their better potentiality to play a significant role in wound healing. All of the selected ligand molecules performed well in the drug likeness property analysis test and ADME/T test but their possibility of metabolism by CYP450 enzymes was poor which may make their chance questionable to be considered a drug. However, further investigation and intervention might be required to improve their metabolism and excretion profile inside the human body. All curcumin analogues showed some significant biological activities in the PASS prediction test which should strengthen their possibility to be considered a drug.

Considering all the parameters of the tests in this experiment it can be concluded that, curcumin I is the best enhancer of CK1 in and curcumin II is the best enhancer of GSK3B in the Wnt signaling pathway. However, other compounds should also be investigated further since they also performed well in docking experiments. Further in vitro and in vivo studies are required to confirm the roles of curcumin analogues in wound healing.

Conclusion

Three curcumins from *Curcuma longa* were utilized in this experiment in a search for a drug to be used in wound healing and injury repair processes. Several tests indicated positive result, suggesting that *Curcuma longa* could be a great source of herbal drug for wound healing and injury repair along with some other diseases as predicted in PASS. Hopefully, this study will raise research interest among researchers.

Acknowledgements
The authors are thankful to the members of the Community of Biotechnology and Swift Integrity Computational Lab, Dhaka, Bangladesh, for the support during the preparation of the manuscript.

Authors' contributions
MA conceived the study. RR, SA, HR, KM, and FR designed the study. RR, MA wrote the draft manuscript. RR, FZ, MI, SR, SO, and MA edited and revised the manuscript. All the authors approved the final version of the manuscript.

Availability of data and materials
All the data are provided within the manuscript.

Declarations

Ethics approval and consent to participate
Not Applicable

Consent for publication
Not Applicable

Competing interests
Riyan Al Islam Reshad, Sayka Alam, Humaira Binte Raihan, Kamrun Nahar Meem, Fatima Rahman, Fardin Zahid, Md. Ikram Rafid, S.M. Obaydur Rahman, Sadman Omit, and Md. Hazrat Ali declare that they have no conflict of interest.

Author details
[1]Department of Genetic Engineering and Biotechnology, Shahjalal University of Science and Technology, Sylhet, Bangladesh. [2]Department of Biotechnology and Genetic Engineering, Jahangirnagar University, Dhaka, Bangladesh. [3]Department of Biochemistry and Microbiology, North South University, Bashundhara, Dhaka, Bangladesh. [4]Department of Genetic Engineering and Biotechnology, University of Chittagong, Chittagong, Bangladesh. [5]Department of Computer Science and Engineering, Shahjalal University of Science and Technology, Sylhet, Bangladesh. [6]Department of Biotechnology and Genetic Engineering, Sylhet Agricultural University, Sylhet, Bangladesh.

Received: 25 January 2021 Accepted: 28 May 2021
Published online: 09 July 2021

References

1. Bowler PG, Duerden BI, Armstrong DG (2001) Wound microbiology and associated approaches to wound management. Clin Microbiol Rev 14(2): 244–269
2. Westgate SJ, Percival SL, Knottenbelt DC, Clegg PD, Cochrane CA (2011) Microbiology of equine wounds and evidence of bacterial biofilms. Vet Microbiol 150(1-2):152–159
3. Whyte JL, Smith AA, Helms JA (2012) Wnt signaling and injury repair. Cold Spring Harb Perspect Biol 4(8):a008078
4. Fathke C, Wilson L, Shah K, Kim B, Hocking A, Moon R, Isik F (2006) Wnt signaling induces epithelial differentiation during cutaneous wound healing. BMC Cell Biol 7(1):4
5. Cheon SS, Nadesan P, Poon R, Alman BA (2004) Growth factors regulate β-catenin-mediated TCF-dependent transcriptional activation in fibroblasts during the proliferative phase of wound healing. Exp Cell Res 293(2):267–274
6. Zamierowski DS, Zamierowski David S (1990) Wound dressing and treatment method. US Patent 4 969:880
7. Pu L (2015) Aesthetic plastic surgery in Asians. Thieme Medical, New York
8. Daryabeigi R, Heidari M, Hosseini SA, Omranifar M (2010) Comparison of healing time of the 2nd degree burn wounds with two dressing methods of fundermol herbal ointment and 1% silver sulfadiazine cream. Iran J Nurs Midwifery Res 15(3):97
9. Budovsky A, Yarmolinsky L, Ben-Shabat S (2015) Effect of medicinal plants on wound healing. Wound Repair Regen 23(2):171–183
10. Chattopadhyay I, Biswas K, Bandyopadhyay U, Banerjee RK (2004) Turmeric and curcumin: biological actions and medicinal applications. Curr Sci Bangalore 87:44–53
11. Jayaprakasha GK, Jagan Mohan Rao L, Sakariah KK (2002) Improved HPLC method for the determination of curcumin, demethoxycurcumin, and bisdemethoxycurcumin. J Agric Food Chem 50(13):3668–3672
12. Demirovic D, Rattan SI (2011) Curcumin induces stress response and hormetically modulates wound healing ability of human skin fibroblasts undergoing ageing in vitro. Biogerontology 12(5):437–444
13. Xiong Y, Zhou L, Su Z, Song J, Sun Q, Liu SS, Xia Y, Wang Z, Lu D (2019) Longdaysin inhibits Wnt/β-catenin signaling and exhibits antitumor activity against breast cancer. Onco Targets Ther 12:993
14. Huang H, He X (2008) Wnt/β-catenin signaling: new (and old) players and new insights. Curr Opin Cell Biol 20(2):119–125
15. Cruciat CM (2014) Casein kinase 1 and Wnt/β-catenin signaling. Curr Opin Cell Biol 31:46–55
16. Polakis P (2000) Wnt signaling and cancer. Genes Dev 14(15):1837–1851
17. Suomalainen M, Thesleff I (2010) Patterns of Wnt pathway activity in the mouse incisor indicate absence of Wnt/β-catenin signaling in the epithelial stem cells. Dev Dyn 239(1):364–372
18. Mao J, Wang J, Liu B, Pan W, Farr GH III, Flynn C, Yuan H, Takada S, Kimelman D, Li L, Wu D (2001) Low-density lipoprotein receptor-related protein-5 binds to Axin and regulates the canonical Wnt signaling pathway. Mol Cell 7(4):801–809
19. MacDonald BT, Semenov MV, He X (2007) SnapShot: Wnt/β-catenin signaling. Cell 131(6):1204–12e1
20. Silkstone D, Hong H, Alman BA (2008) β-Catenin in the race to fracture repair: in it to Wnt. Nat Rev Rheumatol 4(8):413
21. Zhang H, Nie X, Shi X, Zhao J, Chen Y, Yao Q, Sun C, Yang J (2018) Regulatory Mechanisms of the Wnt/β-catenin Pathway in Diabetic cutaneous Ulcers. Front Pharmacol 9:1114
22. Nusse R (2005) Wnt signaling in disease and in development. Cell Res 15(1):28
23. MacDonald BT, Tamai K, He X (2009) Wnt/β-catenin signaling: components, mechanisms, and diseases. Dev Cell 17(1):9–26
24. Kneidinger N, Yildirim AO, Callegari J, Takenaka S, Stein MM, Dumitrascu R, Bohla A, Bracke KR, Morty RE, Brusselle GG, Schermuly RT (2011) Activation of the WNT/β-catenin pathway attenuates experimental emphysema. Am J Respir Crit Care Med 183(6):723–733
25. Baron R, Rawadi G (2007) Targeting the Wnt/β-catenin pathway to regulate bone formation in the adult skeleton. Endocrinology 148(6):2635–2643
26. Bafico A, Gazit A, Pramila T, Finch PW, Yaniv A, Aaronson SA (1999) Interaction of frizzled related protein (FRP) with Wnt ligands and the frizzled receptor suggests alternative mechanisms for FRP inhibition of Wnt signaling. J Biol Chem 274(23):16180–16187
27. Clevers H (2006) Wnt/β-catenin signaling in development and disease. Cell 127(3):469–480
28. Akhmetshina A, Palumbo K, Dees C, Bergmann C, Venalis P, Zerr P, Horn A, Kireva T, Beyer C, Zwerina J, Schneider H (2012) Activation of canonical Wnt signalling is required for TGF-β-mediated fibrosis. Nat Commun 3:735
29. Schrödinger Release 2018-4: Protein Preparation Wizard; Epik, Schrödinger, LLC, New York, NY, 2016; Impact, Schrödinger, LLC, New York, NY, 2016; Prime, Schrödinger, LLC, New York, NY, 2018.
30. Schrödinger Release 2018-4 (2018) LigPrep. Schrödinger, LLC, New York
31. Schrödinger Release 2019-3 (2019) Glide. Schrödinger, LLC, New York
32. Dassault Systèmes BIeOVIA (2019) Discovery Studio Visualizer, 19.1. Dassault Systèmes, San Diego
33. Daina A, Michielin O, Zoete V (2017) SwissADME: a free web tool to evaluate pharmacokinetics, drug-likeness and medicinal chemistry friendliness of small molecules. Sci Rep 7:42717
34. Sander T (2001) OSIRIS property explorer. Organic Chemistry Portal
35. Cheng F, Li W, Zhou Y, Shen J, Wu Z, Liu G, Lee PW, Tang Y (2012) admetSAR: a comprehensive source and free tool for assessment of chemical ADMET properties. J Chem Inf Model 52(11):3099–105. https://doi.org/10.1021/ci300367a. Epub 2012 Nov 1. Erratum in: J Chem Inf Model. 2019;59(11):4959.
36. Rydberg P, Gloriam DE, Olsen L (2010) The SMARTCyp cytochrome P450 metabolism prediction server. Bioinformatics 26(23):2988–2989
37. Filimonov DA, Lagunin AA, Gloriozova TA, Rudik AV, Druzhilovskii DS, Pogodin PV, Poroikov VV (2014) Prediction of the biological activity spectra of organic compounds using the PASS online web resource. Chem Heterocycl Compd 50(3):444–457

38. Lipinski CA, Lombardo F, Dominy BW, Feeney PJ (1997) Experimental and computational approaches to estimate solubility and permeability in drug discovery and development settings. Adv Drug Deliv Rev 23(1-3):3–25
39. Nagori BP, Solanki R (2011) Role of medicinal plants in wound healing. Res J Med Plant 5(4):392–405
40. Kundu S, Biswas TK, Das P, Kumar S, De DK (2005) Turmeric (Curcuma longa) rhizome paste and honey show similar wound healing potential: a preclinical study in rabbits. Int J Low Extrem Wounds 4(4):205–213
41. Purohit SK, Solanki R, Mathur V, Mathur M (2013) Evaluation of wound healing activity of ethanolic extract of Curcuma longa rhizomes in male albino rats. Asian J Pharm Res 3(2):79–81
42. Gohlke H, Hendlich M, Klebe G (2000) Knowledge-based scoring function to predict protein-ligand interactions. J Mol Biol 295(2):337–356
43. Shoichet BK, McGovern SL, Wei B, Irwin JJ (2002) Lead discovery using molecular docking. Curr Opin Chem Biol 6(4):439–446
44. Davis AM, Teague SJ (1999) Hydrogen bonding, hydrophobic interactions, and failure of the rigid receptor hypothesis. Angew Chem Int Ed 38(6):736–749
45. Kadam RU, Roy N (2007) Recent trends in drug-likeness prediction: a comprehensive review of in silico methods. Indian J Pharm Sci 69(5):609
46. Veber DF, Johnson SR, Cheng HY, Smith BR, Ward KW, Kopple KD (2002) Molecular properties that influence the oral bioavailability of drug candidates. J Med Chem 45(12):2615–2623
47. Pollastri MP (2010) Overview on the rule of five. Curr Protoc Pharm 49(1):9–12
48. Leeson PD, Springthorpe B (2007) The influence of drug-like concepts on decision-making in medicinal chemistry. Nat Rev Drug Discov 6(11):881
49. Yu H, Adedoyin A (2003) ADME–Tox in drug discovery: integration of experimental and computational technologies. Drug Discov Today 8(18): 852–861
50. Wang Y, Xing J, Xu Y, Zhou N, Peng J, Xiong Z, Liu X, Luo X, Luo C, Chen K, Zheng M (2015) In silico ADME/T modelling for rational drug design. Q Rev Biophys 48(4):488–515
51. Sarkar B, Alam S, Rajib TK, et al (2021) Identification of the most potent acetylcholinesterase inhibitors from plants for possible treatment of Alzheimer's disease: a computational approach. Egypt J Med Hum Genet 22: 10. https://doi.org/10.1186/s43042-020-00127-8
52. Ullah A, Prottoy NI, Araf Y, Hossain S, Sarkar B, Saha A Molecular docking and pharmacological property analysis of phytochemicals from Clitoria ternatea as potent inhibitors of cell cycle checkpoint proteins in the cyclin/CDK pathway in cancer cells. Comput Mol Biosci 9(03):81
53. Sarkar B, Ullah MA, Johora FT, Taniya MA, Araf Y Immunoinformatics-guided designing of epitope-based subunit vaccine against the SARS Coronavirus-2 (SARS-CoV-2). Immunobiology:151955. https://doi.org/10.1016/j.imbio.2020.151955
54. Ullah A, Sarkar B, Islam SS Exploiting the reverse vaccinology approach to design novel subunit vaccine against ebola virus. Immunobiology:151949. https://doi.org/10.1016/j.imbio.2020.151949
55. Ullah MA, Johora FT, Sarkar B, Araf Y, Rahman MH Curcumin analogs as the inhibitors of TLR4 pathway in inflammation and their drug like potentialities: a computer-based study. J Receptors Signal Transduct:1–5. https://doi.org/10.1080/10799893.2020.1742741
56. Sarkar B, Ullah MA, Islam SS, Rahman MH, Araf Y Analysis of plant-derived phytochemicals as anti-cancer agents targeting cyclin dependent kinase-2, human topoisomerase IIa and vascular endothelial growth factor receptor-2. J Receptors and Signal Transduct. https://doi.org/10.1080/10799893.2020.1805628
57. Paul Gleeson M, Hersey A, Hannongbua S (2011) In-silico ADME models: a general assessment of their utility in drug discovery applications. Curr Top Med Chem 11(4):358–381
58. Li AP (2001) Screening for human ADME/Tox drug properties in drug discovery. Drug Discov Today 6(7):357–366
59. Geerts T, Vander Heyden Y (2011) In silico predictions of ADME-Tox properties: drug absorption. Comb Chem High Throughput Screen 14(5): 339–361
60. Anzenbacher P, Anzenbacherova E (2001) Cytochromes P450 and metabolism of xenobiotics. Cell Mol Life Sci 58(5-6):737–747
61. Trevan JW (1927) The error of determination of toxicity. Proceedings of the Royal Society of London. Proc R Soc Lond B Biol Sci 101(712):483–514
62. Li X, Chen L, Cheng F, Wu Z, Bian H, Xu C, Li W, Liu G, Shen X, Tang Y (2014) In silico prediction of chemical acute oral toxicity using multi-classification methods. J Chem Inf Model 54(4):1061–1069
63. Ames BN, Gurney EG, Miller JA, Bartsch H (1972) Carcinogens as frameshift mutagens: metabolites and derivatives of 2-acetylaminofluorene and other aromatic amine carcinogens. Proc Natl Acad Sci 69(11):3128–3132
64. Xu C, Cheng F, Chen L, Du Z, Li W, Liu G, Lee PW, Tang Y (2012) In silico prediction of chemical Ames mutagenicity. J Chem Inf Model 52(11):2840–2847
65. Parasuraman S (2011) Prediction of activity spectra for substances. J Pharmacol Pharmacother 2(1):52
66. Stepanchikova AV, Lagunin AA, Filimonov DA, Poroikov VV (2003) Prediction of biological activity spectra for substances: Evaluation on the diverse sets of drug-like structures. Curr Med Chem 10(3):225–233
67. Lagunin A, Stepanchikova A, Filimonov D, Poroikov V (2000) PASS: prediction of activity spectra for biologically active substances. Bioinformatics 16(8):747–748
68. Background [Internet]. Smartcyp.sund.ku.dk. 2021. Available from: https://smartcyp.sund.ku.dk/background_smartcyp. Cited 22 January 2021
69. Tyzack JD, Kirchmair J (2019) Computational methods and tools to predict cytochrome P450 metabolism for drug discovery. Chem Biol Drug Des 93(4):377–386

Publisher's Note